

See discussions, stats, and author profiles for this publication at: <https://www.researchgate.net/publication/23403991>

Deposition of Uranium Precipitates in Dolomitic Gravel Fill

ARTICLE *in* ENVIRONMENTAL SCIENCE AND TECHNOLOGY · NOVEMBER 2008

Impact Factor: 5.33 · DOI: 10.1021/es8001579 · Source: PubMed

CITATIONS

11

READS

48

5 AUTHORS, INCLUDING:



[Debra H Phillips](#)

Queen's University Belfast

48 PUBLICATIONS 894 CITATIONS

[SEE PROFILE](#)



[David B Watson](#)

Oak Ridge National Laboratory

153 PUBLICATIONS 3,570 CITATIONS

[SEE PROFILE](#)



[S. D. Kelly](#)

UOP LLIC, A Honeywell Company

120 PUBLICATIONS 3,482 CITATIONS

[SEE PROFILE](#)

Deposition of Uranium Precipitates in Dolomitic Gravel Fill

D. H. PHILLIPS,[†] D. B. WATSON,^{*,‡}
S. D. KELLY,[§] B. RAVEL,[§] AND
K. M. KEMNER[§]

Environmental Engineering Research Centre, School of Planning, Architecture, and Civil Engineering, Queen's University of Belfast, Belfast BT9 5AG, Northern Ireland, UK, Environmental Sciences Division, Oak Ridge National Laboratory, P.O. Box 2008, Oak Ridge, Tennessee 37831, and Molecular Environmental Science Group, Biosciences Division, Argonne National Laboratory, Bldg 203, RM E113, 9700 S. Cass Ave, Argonne, Illinois 60439

Received January 18, 2008. Revised manuscript received June 28, 2008. Accepted July 7, 2008.

Uranium-containing precipitates have been observed in a dolomitic gravel fill near the Department of Energy (DOE) S-3 Ponds former waste disposal site as a result of exposure to acidic ($\text{pH } 3.4$) groundwater contaminated with U (33 mg L^{-1}), Al^{3+} (900 mg L^{-1}), and NO_3^- ($14\,000 \text{ mg L}^{-1}$). The U containing precipitates fluoresce a bright green under ultraviolet (UV) short-wave light which identify U-rich coatings on the gravel. Scanning electron microscopy (SEM) microprobe analysis show U concentration ranges from 1.6–19.8% (average of 7%) within the coatings with higher concentrations at the interface of the dolomite fragments. X-ray absorption near edge structure spectroscopy (XANES) indicate that the U is hexavalent and extended X-ray absorption fine structure spectroscopy (EXAFS) shows that the uranyl is coordinated by carbonate. The exact nature of the uranyl carbonates are difficult to determine, but some are best described by a split K^+ -like shell similar to grimselite [$\text{K}_4\text{Na}(\text{UO}_2)(\text{CO}_3)_3 \cdot \text{H}_2\text{O}$] and other regions are better described by a single Ca^{2+} -like shell similar to liebigite [$\text{Ca}_2(\text{UO}_2)(\text{CO}_3)_3 \cdot 11(\text{H}_2\text{O})$] or andersonite [$\text{Na}_2\text{Ca}\text{UO}_2(\text{CO}_3)_3 \cdot 6\text{H}_2\text{O}$]. The U precipitates are found in the form of white to light yellow cracked-formations as coatings on the dolomite gravel and as detached individual precipitates, and are associated with amorphous basalumnite [$\text{Al}_4(\text{SO}_4)(\text{OH})_{10} \cdot 4\text{H}_2\text{O}$].

Introduction

Radionuclides and other contaminants have been released into the geological material at the Y-12 National Security Complex on the Department of Energy's (DOE) Oak Ridge Reservation (ORR) in Tennessee as a consequence of uranium processing activities, resulting in zones of highly contaminated groundwater and sediments (1). Between 1951 and 1984, high ionic strength nitric acid wastes containing uranium, technetium-99, metals, nitrate, and tetrachloroethylene were disposed in the unlined S-3 ponds which are now capped (2). A large plume of U contaminated groundwater is migrating away from the ponds into nearby Bear

Creek (2, 3). Therefore, it is important to investigate precipitation and adsorption of U to understand and model the fate and transport of U at the site, and to develop and identifying media that will immobilize U from groundwater.

DOE's Oak Ridge Field Research Center (FRC) located at the S-3 Ponds site has been a host for many studies examining the removal of U from groundwater (4–11). For example, Phillips et al. (2, 12) reported U content in the native subsurface geological material near the S-3 ponds as high as 750 mg kg^{-1} at a depth of $\sim 11 \text{ m}$ in interbedded shale and sandstone weathered bedrock at $\text{pH} < 4$. Gu et al. (4) reported coprecipitation of U with mixed solid phases of amorphous Al hydroxides and SO_4^{2-} when FRC site water with $\text{pH} < 4.0$ and high levels of U, Ca^{2+} , Al^{3+} , NO_3^- , and SO_4^{2-} was titrated with NaOH to a $\text{pH} \sim 5.5$. Oxic groundwater conditions prevail at the S-3 site; therefore, hexavalent uranium in the form of an uranyl (UO_2^{2+}) is likely present in the groundwater (4). uranyl carbonates (i.e., UO_2CO_3 and $\text{UO}_2(\text{CO}_3)_2^{2-}$), uranyl nitrates (i.e., $\text{UO}_2\text{NO}_3^{+}$) and uranyl sulfates (i.e., UO_2SO_4 , $\text{UO}_2(\text{SO}_4)_2^{2-}$) may also be present in groundwater depending on localized site specific conditions (13, 14). There is a need to understand uranyl solid phase chemical speciation to determine its solubility, transport properties, and the effectiveness of remediation strategies (15).

The geomedia for this study was collected 60 m from the S-3 Ponds (Figure 1 and Supporting Information Figure S1). Shallow saprolite was excavated and backfilled with dolomite gravel to a depth of about 4 m to construct a base for several large storage tanks (Figure 1). This gravel which was emplaced in 1983 is highly permeable and intercepts approximately the top meter of groundwater plume diverting some of the groundwater contaminants toward Bear Creek (Figure 1). The objectives of this study are to use field, microscopic, molecular, and chemical analyses (1) to examine the geochemical environment which caused the U to precipitate, and (2) to determine the composition/mineralogy of U-containing precipitates within this permeable gravel.

Materials and Methods

Study Area and Geological Materials. The FRC site is underlain by the Nolichucky Shale which is highly contaminated and significantly weathered (to saprolite) to a depth of 15 m. The gravel fill area near the S-3 Ponds where samples were extracted is composed of gray dolomite fragments (2 mm to 3 cm diameter) and fine material ($> 2 \text{ mm}$). XRD and SEM-EDS of the dolomitic gravels and fine material reveal a crystalline mineralogy of dolomite $<$ quartz $<$ calcite $<$ K feldspar $<$ pyrite (Supporting Information Figure S2). The fill extends from the surface down to about 4 m where it interfaces Nolichucky shale saprolite.

Sample Collection, Preparation, and Descriptions. The two cores obtained for this study were collected at the up-gradient terminus of the gravel fill closest to the source area where highly contaminated acidic groundwater first enters the fill. The 4.7 cm diameter continuous cores were collected from the depths of 0–3.66 m (FWB408) and 2.74–3.66 m (FWB410) by a pneumatic hammer-drive coring device. The corer containing a polyurethane tube was driven into the geological material using a Geoprobe drilling rig.

The distribution of the U containing precipitates in polished sections were examined with a short-wave UV lamp and photographed with a Nikon digital camera. U containing precipitates that were generally white to light yellow in natural light were observed as a strongly fluorescent bright green

* Corresponding author phone: (865) 241-4749; fax: (865) 576-8646; e-mail: watsondb@ornl.gov.

[†] Queen's University of Belfast.

[‡] Oak Ridge National Laboratory.

[§] Argonne National Laboratory.

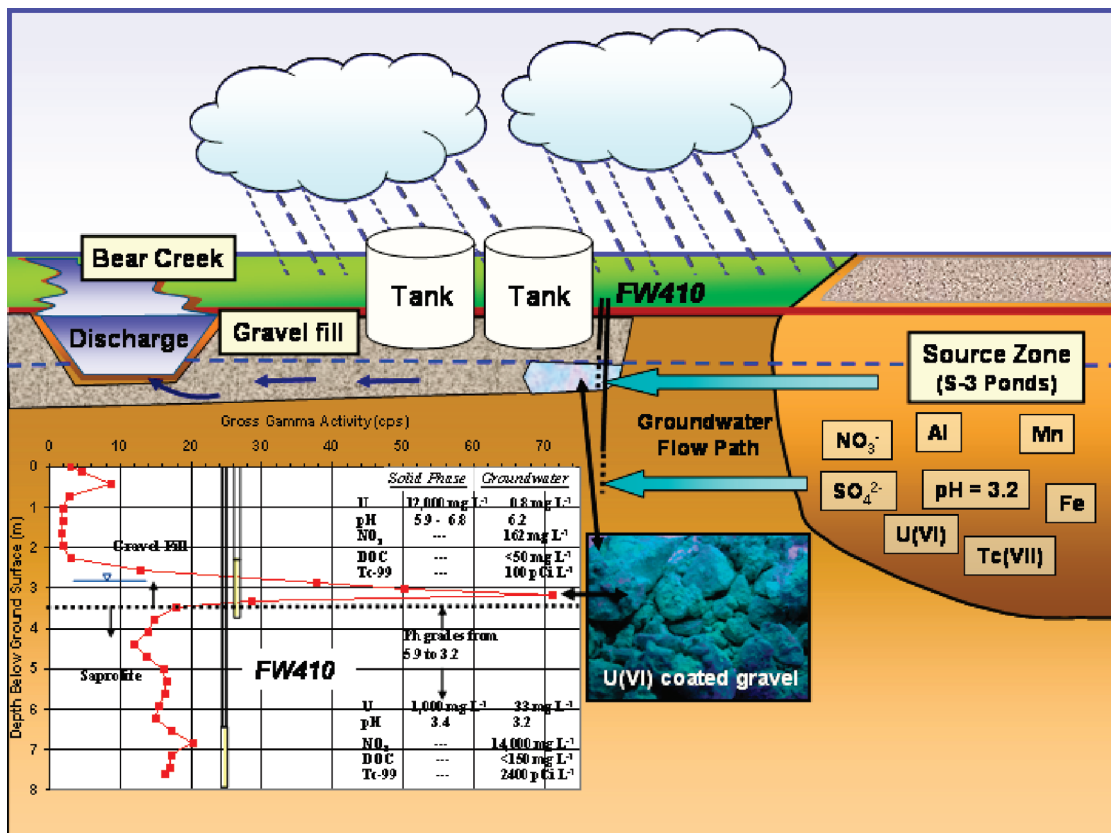


FIGURE 1. Conceptual model of the gravel pathway at the site illustrating the distribution and concentrations of contaminants and related geochemical parameters in the solid and liquid phases. The distribution of the gross gamma activity (CPS-counts/sec) and U, pH, and NO_3^- parameters are shown with depth for groundwater (FW410) and solid phase materials (FW8408). Note dramatic increase in U and gross gamma activity in the carbonate gravel at the interface with the groundwater table. The dolomite fragments fluoresce a bright green under UV light.

under the UV light (Figures 1, 2B, 2D) that distinguished them from other light colored materials within the core sections.

X-ray Diffraction Analysis. Selected dolomite gravel and U precipitates were ground (>80 mesh), then encapsulated in Kapton tape to obtain random orientation of the ground materials. The XRD analysis was performed on a Scientag XDS-2000 X-ray diffractometer (Sunnyvale, CA) using a Rigaku RU-300 Cu rotating anode source (Rigaku, Tokyo, Japan) operating at 50 kV and 100 mA using a Peltier-cooled Si(Li) detector (Scientag, Sunnyvale, CA) and Cu K-alpha radiation.

Microscopic Analyses. Selected undisturbed samples of the core material were impregnated with Hilquist resin (Hilquist, Falls City, WA). After curing, the samples were ground and polished using 1 μm , 0.6 μm , 0.3 μm , and 0.1 μm polishing grit (Buhler LTD, Lake Bluff, IL) and analyzed with a XL30FEG Philips scanning electron microscope (SEM) (Eindhoven, The Netherlands) equipped with backscatter analysis (BSE) and energy dispersive analysis (EDS) at 10kV. SEM-wavelength dispersive spectroscopy (WDS) analysis was performed for 27 h to measure U, Ca^{2+} , Mg^{2+} , S^{2-} , Si , F^- , and Al^{3+} in a selected area in the polished section of a dolomite gravel with uranium containing coatings. SEM-microprobe (Oxford Instruments X-site analyzer) analysis and quantitative line scans (Oxford Instruments X-site analyzer) were taken of selected areas of the coatings to examine the distribution of the elements across the coatings.

X-ray Absorption Spectroscopy (XAS). The X-ray absorption spectroscopy (XAS) spectra measurements were made at the MRCAT (16) beamline at the Advanced Photon Source. The one-dimensional XAS measurements were collected along many lines that transect the gravel-rind interface

(Figure 2, Supporting Information Figure S3 and Table S2) near two gravel pieces labeled G1 (Gravel1) and G2 (Gravel2) and in two areas of the saprolite-dolomitic gravel interface that are labeled G3 (Gravel3) and PF1 (precipitate fragment 1). The X-ray probe size was approximately 0.5 mm both horizontally (including sample orientation of 45°) and vertically. The XAS spectra from the gravel samples is compared to the reference spectra from the mineral grimselite [$\text{K}_3\text{Na}(\text{UO}_2)(\text{CO}_3)_3 \cdot (\text{H}_2\text{O})$] and to previously published liebigite [$\text{Ca}_2(\text{UO}_2)(\text{CO}_3)_3 \cdot 11(\text{H}_2\text{O})$] (17–19). Beamline parameters (S.1) XAS analysis (S.2) and models (S.3) are in the Supporting Information.

Core Material Geochemical Analysis. The pH of the samples were measured using a 1:1 sample:MQ water mixture. The mixture was placed on a box shaker for 30 min then centrifuged at 2100 rpm at 15 min. Gross gamma activity (cps) of the gravel fill and underlying saprolite to a depth of 7.62 m was measured on FWB408 by inserting a NaI gamma detection probe (20) and taking readings every 0.3 m along the length of the borehole.

Groundwater Geochemistry Analysis. Groundwater was sampled from multilevel well FW410 at vertical depths of 4.3 m, screened across the gravel fill, and 8.5 m, screened in the underlying saprolite. Groundwater pH and other field parameters were measured in line (without exposing to the air) in the multilevel wells with a precalibrated Yellow Springs Instruments YSI 63 pH and conductivity probe (Yellow Springs Instruments, CO). Dissolved oxygen (DO) was measured using a Hach HQ40 luminescent DO probe (Hach, Loveland, CO). Sulfate, chloride, and nitrate were analyzed in unacidified groundwater samples with a Dionex 500 ion chromatograph (Dionex, Sunnyvale, CA). Aluminum, Ba^{2+} , Ca^{2+} , K^+ , Mg^{2+} , Na^+ , Mn^{2+} , Sr^{2+} , Si , F^- , and U were analyzed

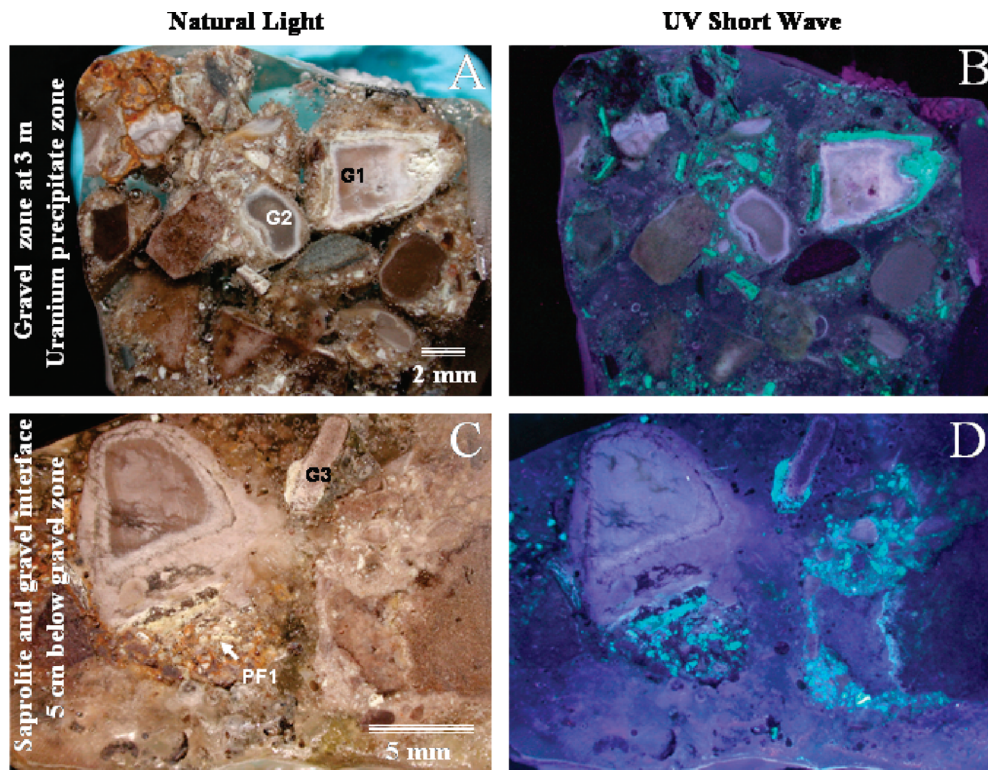


FIGURE 2. Images of polished sections of the U-contaminated zones. (A) Dolomitic gravel: dolomite fragments with light colored weathering rinds and white to light yellow U-containing coatings, and individual U-containing fragments in the surrounding fine material, (B) Figure 2A under UV short wave light where the U-containing coatings and precipitates fluoresce a bright green, (C) Mixed saprolite-gravel interface about 5 cm below the dolomite gravel layer: U-containing coatings (white to light yellow) are on dolomite gravel and individual U-containing fragments are in the clayey saprolite matrix material, and (D) Figure 2C under UV short wave light showing the U-containing material fluorescing a bright green and associated with gravel.

using a Perkin-Elmer Elan 6100 ICP/MS (Perkin-Elmer, Waltham, MA). Groundwater samples collected for metals analysis were filtered with a 0.45 micrometer filter and acidified with HNO_3 to a pH > 2 to preserve the samples.

Results and Discussion

Geochemistry of the U-Enriched Dolomitic Gravel. A shallow layer of carbonate gravel fill intercepts an acidic, high ionic strength, U contaminated groundwater plume (3) increasing the groundwater pH (Supporting Information Table S1) and causing precipitation of U complexes and other minerals in the gravel (Figure 1, Supporting Information Figure S1). Bulk samples in FWB408 below the groundwater table (Figure 1) have a maximum gross gamma activity of 70 cps and the solid phase U of 12 000 mg kg⁻¹. This is a dramatic increase compared to U content of the underlying saprolite (~200 mg kg⁻¹ maximum at 8.5 m). Below the water table, white to light yellow flaky precipitates coat the 2 mm to 5 cm diameter dolomite gravel and also occur as individual precipitates in finer material (>2 mm) found in the gravel interstices (Figures 1, 2A, 2C). Under UV light, these U(VI) containing precipitates strongly fluoresce light green due to high U content (Figures 2B, 2D).

SEM-EDS and microprobe analysis detected S⁻, Al³⁺, U, Si, F⁻, Ca²⁺, and K⁺ in the coatings/precipitates (Figure 3). Brighter zones shown in SEM-WDS elemental maps and higher U content measured by SEM-quantitative (microprobe) line scans confirm higher amounts of U (7.3–19.8% by weight) adjacent to weathering rinds on the dolomite fragments (Figure 3). There are sections within the coatings where U content increases, but they are generally lower than the U content adjacent to the dolomitic gravel. These increases in U content within the coating could be relicts of past groundwater fluctuations. We suggest that the dolomitic

gravel removed less U from the groundwater as the coatings thickened. However, the gravel still remains effective in the removal of U from the contaminant groundwater (average of 7% U throughout coatings). The precipitation of these U containing formations in the gravel has possibly resulted in a dramatic decrease in U content in the shallow groundwater collected from the gravel (Figure 1).

The coatings from the FRC site are similar to the Al³⁺ and SO₄²⁻ rich coatings which form on carbonates used to raise the pH of acid mine drainage waters. Simón et al. (21) report that basalmite coatings precipitated on limestone surfaces that were weathered by the acid waters in pyrite tailings.

SEM-BSE of the gravel reveal that most of the precipitates occur as cracked coatings (up to 2 mm thick) on 2 mm to 3 cm diameter dolomite gravel (Figure 3). The cracking may be due to dehydration during periods when the water table falls. These cracked coatings flake off into the fine material in the gravel interstices and become scattered along with individual U containing precipitates throughout the fine matrix material. Similar cracked coatings are present at other sites in basalmite that formed on limestone grains that were used to increase pH in pyrite tailings (21).

The shallow port of well FW410 screened in the gravel had U and Tc-99 concentrations of 0.81 mg L⁻¹ and 98 pCi L⁻¹ compared to 40 mg L⁻¹ and 2400 pCi L⁻¹ detected in the sampling port screened in the underlying highly contaminated saprolite (Figure 1). There were notable decreases in NO₃⁻, Al³⁺, Cl⁻, K⁺, Ca²⁺, Mg²⁺, Na⁺, Mn²⁺, Sr²⁺, and F⁻ groundwater concentrations in the shallow gravel zone compared to their concentrations in the underlying shale, while the pH of groundwater and solid phase samples increased in the gravel compared to the underlying shale saprolite (Supporting Information Table S1; Figure 1). Solid phase Al³⁺ and Si in the coatings averaged 43% and 0.8%,

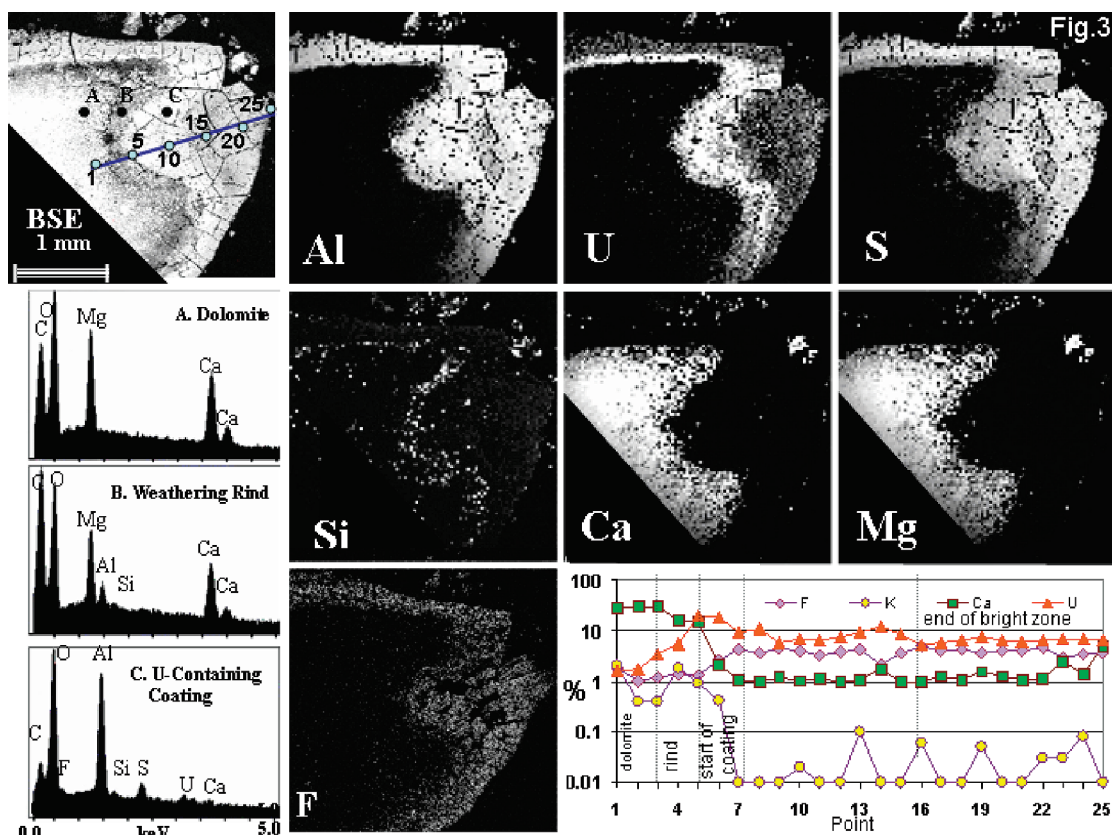


FIGURE 3. SEM-BSE-EDS, elemental mapping (WDS) and line scan microprobe analysis of a section of dolomite with the weathering rind and U-containing coating from Figure 2A. Note that U and K^+ concentrations increase adjacent to the weathering rind, and K^+ is not mapped.

respectively. The high level of Al^{3+} and Si concentrations in the groundwater results from the acidic groundwater weathering the naturally occurring alumino-silicates in the shale saprolite. Phillips et al. (2) report a high correlation of U and Al^{3+} ($r^2 = 0.98$) in groundwater in the adjacent Area 3. Sulfur averages 1.35% in the precipitates. The higher SO_4^{2-} concentration in the groundwater in the gravel compared to the shale (Supporting Information Table S1) could be due to the weathering of pyrite (FeS_2) inclusions in the dolomite (Supporting Information Figure S2) and in the fine material in the gravel layer. The F^- detected in the precipitates (ave. 4.2%, ranging 1.3–7.0%) by SEM microprobe are a result of past waste disposal activities at the S-3 Ponds. Deposits of K^+ occurred in minor amounts, averaging 0.10% (ranged 0–4.7%) in the precipitates with the highest concentrations at the interface of the weathering rind where the U concentrations are elevated. Microprobe detected Ca^{2+} at an average of 1.5% (range 1.0–5.7%) in the precipitates; however, Ca^{2+} and Mg^{2+} were not observed in the coatings by SEM-WDS mapping due to dramatically higher amounts in the dolomite gravel fragments.

Identification of the Uraniferous Precipitates. The normalized XANES spectra from G1-region (at $y = -1000$ $x = -4000$) (Supporting Information Figures S3A, 4A) shows the shape of the absorption edge is nearly identical to the U(VI) standard indicating hexavalent U similar to the uranyl carbonate standard (Figures 4B, 4C). All 80 of the XANES spectra collected along the gravel-rind transect lines (Supporting Information Figure S3) are similar to the G1-region spectra shown.

The U EXAFS spectra (Figure 4D) illustrates the similarity of the grimselite spectrum to the G1- and G3-regions (at spectra $y = -1000$, $x = -4000$) (Supporting Information Figure S3B) with a maximum in the spectra at $\sim 3 \text{ \AA}^{-1}$, 5 \AA^{-1} , 9.8 \AA^{-1} , and 12 \AA^{-1} . All spectra have a broad flat region from 6.5 \AA^{-1}

to 8 \AA^{-1} . These general features indicate bidentate bonding as shown for the carbonate moiety (Figures 4B and C) (17, 19) where the uranyl is bonded to two oxygen atoms of the carbonate group (Supporting Information Figures S4–S6). The measured grimselite spectrum and model (Figures 4D and F), the EXAFS model (Supporting Information), and the model parametrization (Supporting Information Tables S3 and S4) are typical for a uranyl carbonate (17–19) as well as grimselite (22).

EXAFS results indicate two different types of uranyl carbonate minerals (Figures 4D–F) were present within amorphous basalumite coatings and precipitates in the dolomitic gravel (Supporting Information Figures S3, S7–S9; Tables S2, S3, S5–S10). Representative Fourier transforms of a spectrum from the G1-region modeled with a split K^+ shell and from the G3-region modeled with a single Ca^{2+} shell are shown in Figures 4D–F.

The uranyl carbonate in $K_4[UO_2(CO_3)_3]$ is coordinated by six K^+ cations at two different distances making up the split K^+ shell (similar to Figure 4B). The uranyl carbonate in liebigite and andersonite is coordinated by 2 Ca^{2+} cations (Figure 4C). It is not possible to determine the exact mineral structure of the uranyl carbonate minerals in the precipitates from the gravel zone. It is likely that a variety of cations such as Na^+ , K^+ , Cs^+ , Mg^{2+} , Ca^{2+} , Sr^{2+} , Ba^{2+} , and Cu^{2+} are incorporated into the uranyl carbonates. The EXAFS spectra are sensitive to the distances to and the splitting of these cations such that the spectra modeled with a split K^+ -like shell is distinct from the spectra modeled with a single Ca^{2+} -like shell. However, theoretical simulations of the EXAFS spectra for rutherfordine, a pure uranyl carbonate, was not consistent with the measured spectra, indicating that some additional cations are part of the uranyl carbonate precipitate. The groundwater chemistry (Supporting Information Table S1) suggests that many different cations could be incorpo-

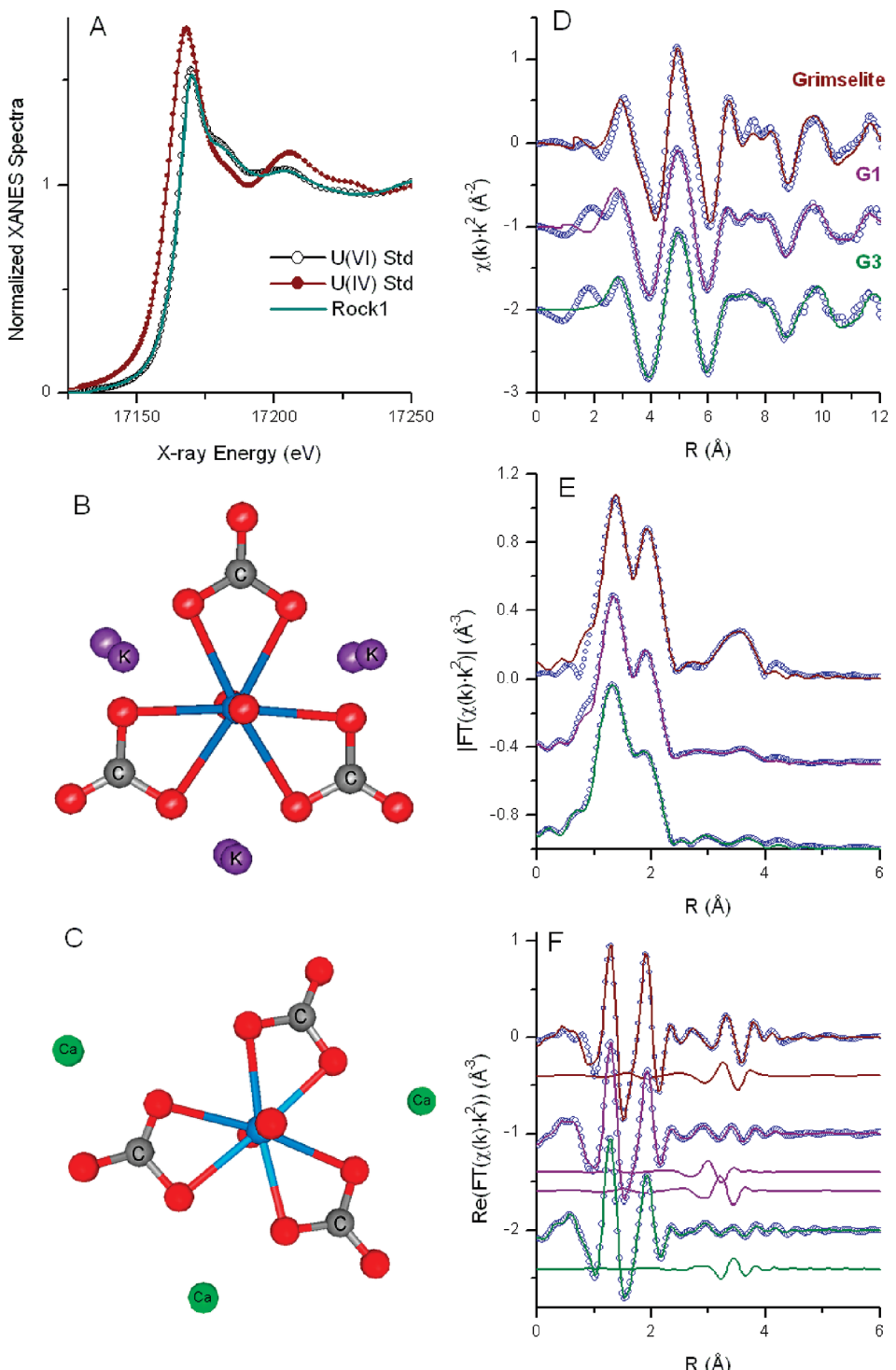


FIGURE 4. U L_{III} -edge XAS spectra and models. (A) Normalized U L_{III} -edge XANES spectra from a U(VI) standard, a U(IV) standard and the sample from the G1-region. The absorption edge of the U(IV) standard is to the left (at lower X-ray energy) of the U(VI) standard and the G1-region spectra. (B and C) The grimselite structure with six K atoms and the liebigite structure with two Ca atoms, respectively. The blue, red, grey, purple and green spheres represent U, O, C, K, and Ca atoms, respectively. (D–F) U L_{III} -edge $\chi(k) \cdot k^2$ spectra (D), magnitude of the Fourier transform (E), and real part of the Fourier transform (F). In panels D–F the measured spectra are shown as symbols and models are shown as solid lines for grimselite standard (top), G1-region (middle), and G3-region (bottom). Panel F also shows the contribution to the model from a single K^+ shell model for the grimselite standard (top), the split K^+ shells model for G1-region (middle), and the single Ca^{2+} shell model for G3-region (bottom).

rated into the precipitate coatings as shown in Figure 4. XRD was unable to confirm the presence of these uranyl carbonates due to detection limits (>5%).

Distribution of Uranyl Carbonates in the Precipitates. EXAFS results indicate uranyl carbonates with a split K^+ -like shell directly adjacent to the weathering rinds, possibly as

thin surface coatings on the gravel where U and K^+ concentrations were highest in the coatings (Supporting Information Figure S3; Table S2). However, this is not always the case. Uranyl carbonates with a single Ca^{2+} -like shell was detected throughout the coating on a gravel fragment from the gravel-saprolite interface. Both uranyl carbonates were

detected in the precipitates in the fine material (>2 mm fraction) from the gravel section and gravel–saprolite interface section. Although the total number of K⁺ atoms was constrained to six, the number of K⁺ atoms within two subshells for all the spectra did not change significantly for most regions (G1, G2, and PF-1). The coordination values for the first K (i.e., K1) shell were 2.3 ± 0.1 to 2.5 ± 0.1 , and those for the precipitate fragments within the PF1–2 group were 1.8 ± 0.2 (Supporting Information Table S8). The σ^2 values for the U–K coordination shells for the PF1–2 group are slightly larger than those for the other regions (0.013 ± 0.003 Å² versus an average value of 0.009 ± 0.002 Å²) (Supporting Information Table S8). The difference in the distribution of K⁺ atoms between the two coordination shells and the difference in the σ^2 values for the PF1–2 region, compared to all the other regions measured, could be an indication of slightly different geochemical conditions during the formation of these flaked off precipitates or a transformation following formation since the flaked off regions have higher surface area and, hence, a different reactivity.

Implications for Carbonates in the Sequestration of Uranium from Acidic Contaminated Groundwater. This study illustrates that carbonate minerals such as dolomite can remove U from acidic contaminated groundwater with high levels of Al³⁺, Ca²⁺, NO₃⁻, and SO₄²⁻ by raising the groundwater pH which induces precipitation of U, similar to a number of other media, such as zerovalent iron (5, 6), synthetic resin (7, 23, 24), and apatite (25, 26). Therefore, carbonate gravel could be considered as an alternative medium for the removal and sequestration of U from contaminated groundwater. However, it is expected that some passivation and decrease in reactivity will occur as the thickness of the precipitates increases on the surface of the carbonate medium. Our study showed that as the U-enriched coatings thickened, the concentration of U within the coatings generally decreased. Similarly, Simón et al. (21) reported that the limestone grains initially raised the pH of pyrite tailings groundwater, but as the limestone became continuously coated with basalmite, they became less effective in raising the pH of the groundwater. They suggested disturbing the limestone grains to break off the coatings to increase the reactivity. Field studies are needed to further determine the capacity of this medium to remove U from groundwater and the potential for remobilization. Furthermore, the remaining dissolved phase U in the gravel (~1 mg L⁻¹), although more than an order of magnitude lower than groundwater concentrations in the saprolite (~40 mg L⁻¹), is possibly a uranyl carbonate form which tends to be highly mobile under the geochemical conditions found in the high pH gravel zone. Although additional studies are needed to better understand the long-term sequestration of U in the precipitates detected at the FRC site, these initial field studies indicate the promise of carbonate minerals such as dolomite for the removal of U from acidic groundwater.

Acknowledgments

The submitted manuscript has been authored by a contractor of the U.S. Government under contract No. DE-AC05-96R22464. This work was supported by the DOE, Office of Science, Environmental Remediation Science Program. Kenneth Lowe, Kirk Hyder, and George Houser assisted in the collection and analysis of cores and groundwater samples. Brian Spalding measured the gross gamma activity. We are grateful to Kathryn E. Fenske for aligning and averaging the EXAFS spectra and to Maxim I. Boyanov for preparing and characterizing the grimselite standard. Use of the Advanced Photon Source was supported by the DOE, Office of Science, Office of Basic Energy Sciences, under Contract No. DE-AC02-06CH11357. MRCAT operations are supported by the DOE and the MRCAT member institutions.

Supporting Information Available

A description of the MR-CAT beamline parameters (S.1), the X-ray Absorption Analysis Methods (S.2), the EXAFS model (S.3) and references. This material is available free of charge via the Internet at <http://pubs.acs.org>.

Literature Cited

- (1) ORNL. the Chemical and Radiological Characterization of the S-3 Ponds, ORNL TM Report. Y/MA-6400;Oak Ridge National Laboratory: Oak Ridge, TN, 1984.
- (2) Phillips, D. H.; Watson, D. B.; Roh, Y.; Mehlhorn, T. L.; Moon, J.-W.; Jardine, P. M. Distribution of uranium contamination in weathered fractured saprolite/shale and contaminated groundwater. *J. Environ. Qual.* **2006**, *35*, 1715–1730.
- (3) Watson, D. B.; Doll, W. E.; Gamey, T. J.; Sheehan, J. R.; Jardine, P. M. Plume and lithological profiling with surface resistivity and seismic tomography. *Groundwater* **2005**, *43*, 169–177.
- (4) Gu, B.; Brooks, S. C.; Roh, Y.; Jardine, P. M. Geochemical reactions and dynamics during titration of a contaminated groundwater with high uranium, aluminum and calcium. *Geochim. Cosmochim. Acta* **2003**, *67*, 2749–2761.
- (5) Phillips, D. H.; Gu, B.; Watson, D. B.; Roh, Y.; Liang, L.; Lee, S. Y. Performance evaluation of a zerovalent iron reactive barrier: Mineralogical characteristics. *Environ. Sci. Technol.* **2000**, *34*, 4169–4176.
- (6) Phillips, D. H.; Watson, D. B.; Roh, Y.; Gu, B. Mineralogical characteristics and transformations during long-term operation of a zero-valent iron reactive barrier. *J. Environ. Qual.* **2003**, *32*, 2033–2045.
- (7) Phillips, D. H.; Gu, B.; Watson, D. B.; Parmele, C. S. Uranium removal from contaminated groundwater by synthetic resins. *Water Res.* **2008**, *42*, 260–268.
- (8) Luo, J.; Wu, W.-M.; Carley, J.; Ruan, C.; Gu, B.; Jardine, P. M.; Criddle, C. S.; Kitanidis, P. K. Hydraulic performance analysis of a multiple injection-extraction well system. *J. Hydrol.* **2007**, *336*, 294–302.
- (9) Luo, J.; Wu, W.-M.; Fienen, M. N.; Jardine, P. M.; Mehlhorn, T. L.; Watson, D. B.; Cirpka, O. A.; Criddle, C. S.; Kitanidis, P. K. 2006. A nested cell approach for in situ remediation. *Groundwater* **2006**, *44*, 266–274.
- (10) Wu, W.; Carley, J.; Luo, J.; Ginder-Vogel, M. A.; Cardenas, E.; Leigh, M. B.; Hwang, C.; Kelly, S. D.; Ruan, C.; Wu, L.; Van Nostrand, J.; Gentry, T.; Lowe, K.; Mehlhorn, T.; Carroll, S.; Lou, W.; Fields, W.; Gu, B.; Watson, D.; Kemner, K. M.; Marsh, T.; Tiedje, J.; Zhou, J.; Fendorf, S.; Kitanidis, P. M.; Jardine, P. M.; Criddle, C. S. In-situ bioreduction of uranium (VI) to submicromolar levels and reoxidation by dissolved oxygen. *Environ. Sci. Technol.* **2007**, *41*, 5716–5723.
- (11) Istok, J. D.; Senko, J. M.; Krumholz, L. R.; Watson, D.; Bogle, M. A.; Peacock, A.; Chang, Y. J.; White, D. C. In situ bioreduction of technetium and uranium in a nitrate-contaminated aquifer. *Environ. Sci. Technol.* **2004**, *38*, 468–475.
- (12) Phillips, D. H.; Watson, D. B.; Roh, Y. Uranium deposits in a weathered fractured saprolite/shale. *Environ. Sci. Technol.* **2007**, *41*, 7653–7660.
- (13) Couston, L.; Pouyat, D.; Moulin, C.; Decambox, P. Speciation of uranyl species in nitric acid medium by time-resolved laser-induced fluorescence. *Appl. Spectrosc.* **1995**, *49*, 349–353.
- (14) Mauline, C.; Decambox, P.; Decaillon, J. G. Uranium speciation in solution by time-resolved laser-induced fluorescence. *Anal. Chem.* **1995**, *67*, 348–1998.
- (15) Kelly, S. D.; Kemner, K. M.; Carley, J.; Criddle, C.; Jardine, P. M.; Marsh, T. L.; Phillips, D.; Watson, D.; Wu, W.-M. Speciation of uranium in sediments before and after in situ bioreduction. *Environ. Sci. Technol.* **2008**, *42*, 1558–1564.
- (16) Segre, C. U.; Leyarovska, N. E.; Chapman, L. D.; Lavender, W. M.; Plag, P. W.; King, A. S.; Kropf, A. J.; Bunker, B. A.; Kemner, K. M.; Dutta, P.; Druan, R. S.; Kaduk, J. The MRCAT insertion device beamline at the Advanced Photon Source. *Synchrotron Radiat. Inst* **2000**, *CP521*, 419–422.
- (17) Catalano, J. G.; Brown, G. E. Analysis of uranyl-bearing phases by EXAFS spectroscopy: Interferences, multiple scattering, accuracy of structural parameters, and spectral differences. *Am. Mineral.* **2004**, *89*, 1004–1021.
- (18) Amayri, S.; Reich, T.; Arnold, T.; Geipel, G.; Bernhard, G. 2005. Spectroscopic characterization of alkaline earth uranyl carbonates. *J. Solid State Chem.* **2005**, *178*, 567–577.
- (19) Kelly, S. D.; Kemner, K. M.; Brooks, S. C. X-ray absorption spectroscopy identifies calcium-uranyl-carbonate complexes

- at environmental concentrations. *Geochim. Cosmochim. Acta* **2007**, *71*, 821–834.
- (20) Miller, K. M.; Shebell, P.; Klemic, G. A. In situ gamma-ray spectroscopy for the measurement of uranium in surface soils. *Health Physics* **1994**, *67*, 140–150.
- (21) Simón, M.; Martin, F.; García, I.; Bouza, P.; Dorronsoro, C.; Aguilar, J. Interaction of limestone grains and acidic solutions from the oxidation of pyrite tailings. *Environ. Pollut.* **2005**, *135*, 65–72.
- (22) Allen, P. G.; Bucher, J. J.; Clark, D. L.; Edelstein, N. M.; Ekberg, S. A.; Gohdes, J. W.; Hudson, E. A.; Kaltsoyannis, N.; Lukens, W. W.; Neu, M. P.; Palmer, P. D.; Reich, T.; Shuh, D. K.; Tait, C. D.; Zwick, B. D. Multinuclear NMR, Raman, EXAFS, and X-ray-diffraction studies of uranyl carbonate complexes in near-neutral aqueous-solution: X-ray Structure of $[C(NH_2)_3]_6[(UO_2)_3(CO_3)_6]6.5H_2O$. *Inorg. Chem.* **1995**, *34*, 4797–4807.
- (23) Gu, B.; Ku, Y.-K.; Jardine, P. M. 2004. Sorption and binary exchange of nitrate, sulfate, and uranium on an anion-exchange resin. *Environ. Sci. Technol.* **2004**, *38*, 3184–3188.
- (24) Gu, B.; Ku, Y.-K.; Brown, G. M. Sorption and desorption of perchlorate and U(VI) by strong-base anion-exchange resins. *Environ. Sci. Technol.* **2005**, *39*, 901–907.
- (25) Fuller, C. C.; Bargar, J. R.; Davis, J. A.; Piana, M. J. Mechanisms of uranium interactions with hydroxyapatite: implications for groundwater remediation. *Environ. Sci. Technol.* **2002**, *36*, 158–165.
- (26) Fuller, C. C.; Bargar, J. R.; Davis, J. A. Molecular-scale characterization of uranium sorption by bone apatite materials for a permeable reactive barrier demonstration. *Environ. Sci. Technol.* **2003**, *37*, 4642–4649.

ES8001579